Atmos. Chem. Phys., 10, 5001–5010, 2010
www.atmos-chem-phys.net/10/5001/2010/
doi:10.5194/acp-10-5001-2010

Atmospheric Chemistry and Physics

Aerosol-induced changes of convective cloud anvils produce strong climate warming

I. Koren[1], L. A. Remer[2], O. Altaratz[1], J. V. Martins[2,3], and A. Davidi[1]

[1]Department of Environmental Sciences Weizmann Institute, Rehovot 76100, Israel
[2]Laboratory for Atmospheres, NASA Goddard Space Flight Center, Greenbelt, Maryland, USA
[3]Department of Physics and Joint Center for Earth Systems Technology, University of Maryland Baltimore County, USA

Received: 7 January 2010 – Published in Atmos. Chem. Phys. Discuss.: 25 January 2010
Revised: 22 May 2010 – Accepted: 26 May 2010 – Published: 31 May 2010

Abstract. The effect of aerosol on clouds poses one of the largest uncertainties in estimating the anthropogenic contribution to climate change. Small human-induced perturbations to cloud characteristics via aerosol pathways can create a change in the top-of-atmosphere radiative forcing of hundreds of Wm^{-2}. Here we focus on links between aerosol and deep convective clouds of the Atlantic and Pacific Intertropical Convergence Zones, noting that the aerosol environment in each region is entirely different. The tops of these vertically developed clouds consisting of mostly ice can reach high levels of the atmosphere, overshooting the lower stratosphere and reaching altitudes greater than 16 km. We show a link between aerosol, clouds and the free atmosphere wind profile that can change the magnitude and sign of the overall climate radiative forcing.

We find that increased aerosol loading is associated with taller cloud towers and anvils. The taller clouds reach levels of enhanced wind speeds that act to spread and thin the anvil clouds, increasing areal coverage and decreasing cloud optical depth. The radiative effect of this transition is to create a positive radiative forcing (warming) at top-of-atmosphere.

Furthermore we introduce the cloud optical depth (τ), cloud height (Z) forcing space and show that underestimation of radiative forcing is likely to occur in cases of non homogenous clouds. Specifically, the mean radiative forcing of towers and anvils in the same scene can be several times greater than simply calculating the forcing from the mean cloud optical depth in the scene.

Limitations of the method are discussed, alternative sources of aerosol loading are tested and meteorological variance is restricted, but the trend of taller clouds, increased and thinner anvils associated with increased aerosol loading remains robust through all the different tests and perturbations.

Correspondence to: I. Koren
(ilan.koren@weizmann.ac.il)

1 Introduction

Increase in aerosol concentration may invigorate convective clouds through the particles' role as cloud condensation nuclei (CCN) and the related feedbacks ignited by changes of the clouds' initial droplet size distribution (Andreae et al., 2004; Koren et al., 2005). The proposed chain of events links initial changes in the size distribution of the cloud's droplets to changes in the net updraft velocities, droplet growth rates, cloud vertical development and precipitation in the warm, mixed and cold phases.

Previous studies show clear correlations between cloud coverage, lifetime (Albrecht, 1989; Jacobson et al., 2007; Kaufman and Koren, 2006) and optical properties (Twomey, 1977; Rosenfeld, 2000). It was shown from satellite data analysis and in situ measurements, that for convective clouds, increase in aerosol loading is associated with taller invigorated clouds, larger cloud fraction and more extensive ice portions. These associations are found over the tropical Atlantic (Koren et al., 2005; Jenkins and Pratt, 2008; Jenkins et al., 2008), Europe (Devasthale et al., 2005), North and South America (Andreae et al., 2004; Koren et al., 2008a; Lindsey and Fromm, 2008), and appear for all types of aerosol particles: biomass burning smoke, urban/industrial aerosol and desert dust. Numerical modeling studies show aerosols

Published by Copernicus Publications on behalf of the European Geosciences Union.

penetrating cloud base of maritime clouds dramatically increasing the amount of supercooled water, as well as the ice contents and vertical velocities (Khain et al., 2008a, b). Aerosol particles can also affect convective cloud properties when ice nucleating particles are entrained directly into the ice portion of the cloud (Fridlind et al., 2004).

Deep convective clouds consist of the cloud tower (or towers) where most of the convection occurs and the cloud anvil (or anvils), which is a thinner layer of mostly ice particles extending away from the cloud towers. Anvils form when part of the cloud spreads out below a stable atmospheric (inversion) layer, such as the tropopause. The anvil horizontal area can be much larger than the tower area, as the inversion layer above it acts as a ceiling, blocking the anvil cloud elements from expanding upwards and forcing horizontal expansion. The anvil elements are further spread by the horizontal winds below the inversion level (Fig. 1a).

Over the tropical Atlantic, convective cloud liquid water optical depth and ice optical depth respond differently to increase in aerosol loading (measured by the aerosol optical depth, AOD) as observed from satellites (Koren et al., 2005). As expected, due to changes in the droplet size-distribution and warm rain suppression, liquid cloud optical depth increases with AOD, however, ice cloud optical depth decreases. Here by analyzing horizontal wind profiles from radiosonde data from several stations in the tropics and subtropics (NOAA/ESRL Radiosonde Database), cloud and aerosol level-3 MODIS version 5, daily data (MODIS – Moderate Resolution Imaging Spectroradiometer, Platnick et al., 2003; Remer et al., 2008), we show that the clear reduction in the average ice optical depth with increase in aerosol loading is due to a strong increase in the ice anvil area. We then estimate the anvil enhancement consequences to the climate radiative balance using a tropical profile (Ricchiazzi et al., 1998). The study area focuses on the tropical Atlantic (0° N to 14° N; 18° W to 45° W) and tropical Pacific (0° N to 14° N; 180° W to 150° W) of June-July-August 2007 using the MODIS-Aqua data (01:30 p.m. local-time overpass).

2 Analysis and results

2.1 MODIS data

We introduce the Tower to Anvil area ratio (TAR), and show that while clouds are invigorated by increasing aerosol loading and reach higher levels in the atmosphere, this ratio decreases due to the associated increase and spread of the anvil area. The anvil area increases both due to the enhanced convection and stronger horizontal winds in the upper troposphere. Figure 1b shows a whole month average (August) daytime horizontal wind speed of the free atmosphere (above the boundary layer) as a function of pressure level for 3 stations along the tropical Atlantic: Natal, Brazil (5.9° S 35.2° W); Ilha Fernando de Noronha, Brazil (3.8° S 32.4° W), Ascension Island (7.9° S 14.4° W). A consistent sharp increase with height occurs from 300 to 150 hPa (~9 to 15 km) and then decreases towards the tropopause (100 hPa). This behavior is consistent for the wide variety of stations analyzed (day and night, land and ocean, inside and outside the tropics, for all seasons). The high level jet contributes to spreading and diluting the anvils, expanding the total cloud cover and decreasing the TAR.

The link between cloud fraction and cloud height (measured as cloud top pressure) over the Atlantic study area is shown in Fig. 1c. Indeed it is shown that the average cloud fraction (each point is an average of 60 one-degree MODIS pixels after sorting all pixels by their cloud top pressure values) increases as a function of the cloud top height. The change in slope at ~850 hPa marks the transition from the lower (marine boundary layer) to the free – upper troposphere where the clouds have larger average fraction. At 300 hPa almost complete overcast conditions are reached.

How does aerosol loading affect the dependence of cloud fraction and height? After filtering out shallow clouds (cloud tops below 800 hPa), the cloud fraction data over the Atlantic was sorted according to the aerosol optical depth (AOD) and divided into 3 equally-sampled groups with mean AOD of each group equal to 0.13, 0.24, 0.41, respectively. Then the same analysis described for Fig. 1c was done for each subgroup (see for more details: Koren et al., 2005, 2008a). While the cloud fraction of all 3 groups increases as a function of the pressure level, a clear shift of the polluted clouds towards larger fraction is shown for each pressure level. Moreover the invigoration effect is also shown as the polluted clouds are taller (Fig. 1d).

MODIS retrieves detailed cloud and aerosol properties with resolution of 1 to 10 km. The data are averaged into a daily 1° resolution grid allowing for simultaneous observations of aerosols in cloud-free regions and clouds in the cloudy regions of the grid box when not completely overcast. To save the information of the higher resolution retrievals (1 km^2 for clouds and 10 km^2 for aerosol) histograms of the original cloud and aerosol properties are provided (King et al., 2003). The histograms of the ice cloud optical depth (τ) were analyzed as a function of the AOD over the study areas. After inspection of many high resolution anvil optical depth data over the region and based on the cloud optical depth distribution (Fig. 2), we divided the histograms into two regimes: anvil ($\tau < 10$) and tower ($\tau > 10$). The Tower to Anvil area ratio (TAR) is the averaged number of pixels in the tower regime (N_t) divided by the number of pixels in the anvil regime (N_a):

$$\mathrm{TAR} = \frac{N_t}{N_a} \quad (1)$$

The average cloud optical depth τ_c is weighted by the horizontal coverage area of the anvil optical depth (τ_a) and the tower optical depth (τ_t):

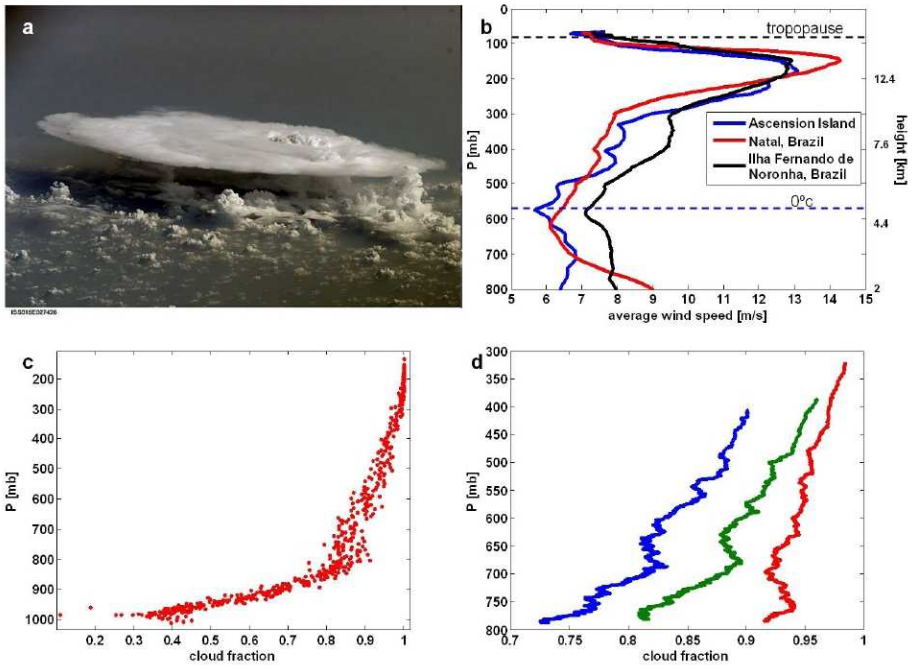

Fig. 1. (a) Photograph of a deep convective cloud with large anvil over Africa – 5 February 2008, photographed from the space shuttle (Image courtesy of the Image Science & Analysis Laboratory, NASA Johnson Space Center). **(b)** Monthly average daytime wind profiles measured with radiosondes at 3 stations along the tropical Atlantic: Natal, Brazil (red, 5.9° S 35.2° W); Ilha Fernando de Noronha, Brazil (black, 3.8° S 32.4° W), Ascension Island (blue, 7.9° S 14.4° W). **(c)** Analysis of cloud fraction as a function of the cloud top pressure (height) over the ITCZ (tropical Atlantic). **(d)** Focusing on the free atmosphere (>800 hPa), cloud fraction as a function of the cloud top pressure for 3 averaged aerosol groups, AOD=0.13 (blue), 0.24 (green) and 0.41 (red), for the tropical Atlantic. Note that the pressure level ranges (height) are different for b, c and d.

$$\tau_c = \frac{N_t \tau_t + N_a \tau_a}{N_t + N_a} = \frac{\mathrm{TAR} \cdot \tau_t + \tau_a}{\mathrm{TAR} + 1} \quad (2)$$

As the TAR becomes smaller, τ_a contributes more to the total cloud optical depth τ_c. Figure 3a shows that the TAR decreases significantly (from ~0.6 to ~0.35) for an average AOD variation from clean ~0.1 to polluted 0.3. Furthermore, Fig. 3b shows that the average ice cloud fraction increases significantly as a function of the AOD and that most of the increase is in the anvil area. Figure 3c shows that as the aerosol loading increases, the anvil height increases and the anvil optical depth decreases significantly. The same analyses are shown for the Pacific dataset in Fig. 3d to f, but for a smaller AOD range (0.05>AOD>0.2) more appropriate for the less aerosol-laden Pacific. Over the Atlantic we repeated the analysis using 2002 MODIS Terra (10:30 a.m. local-time overpass) and 2005 Aqua data. The trends were similar in all years both for Terra and Aqua.

The proposed chain of events suggested here is the following: aerosols serving as CCNs invigorate convection and increase the cloud vertical extent into the upper troposphere (Fig. 1d, 3c and 3f). The taller clouds now reach higher in the atmosphere and spread horizontally, aided by the stronger winds aloft (Fig. 1b), and result in higher (mostly anvil) cloud fraction (Figs. 1d, 3b and e). As the wind shear

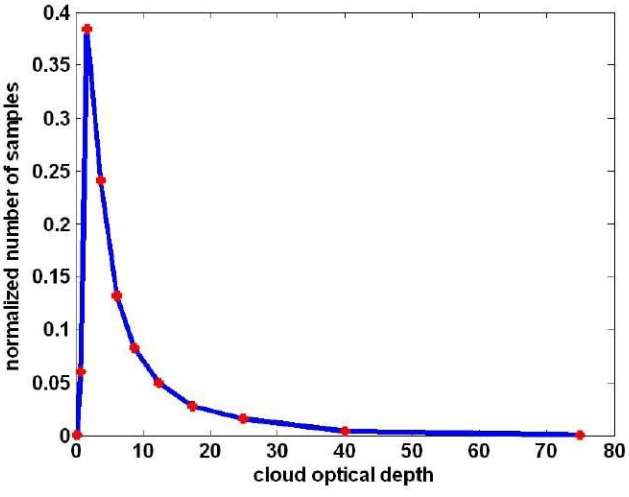

Fig. 2. The histogram of the ice cloud optical depth (τ) values over the Atlantic study area. The red dots mark the MODIS histogram bins. A τ range between 6 to 18 was tested as a threshold between anvils to towers and all threshold showed the same trend. Throughout this study τ=10 was selected as the threshold between tower and anvils.

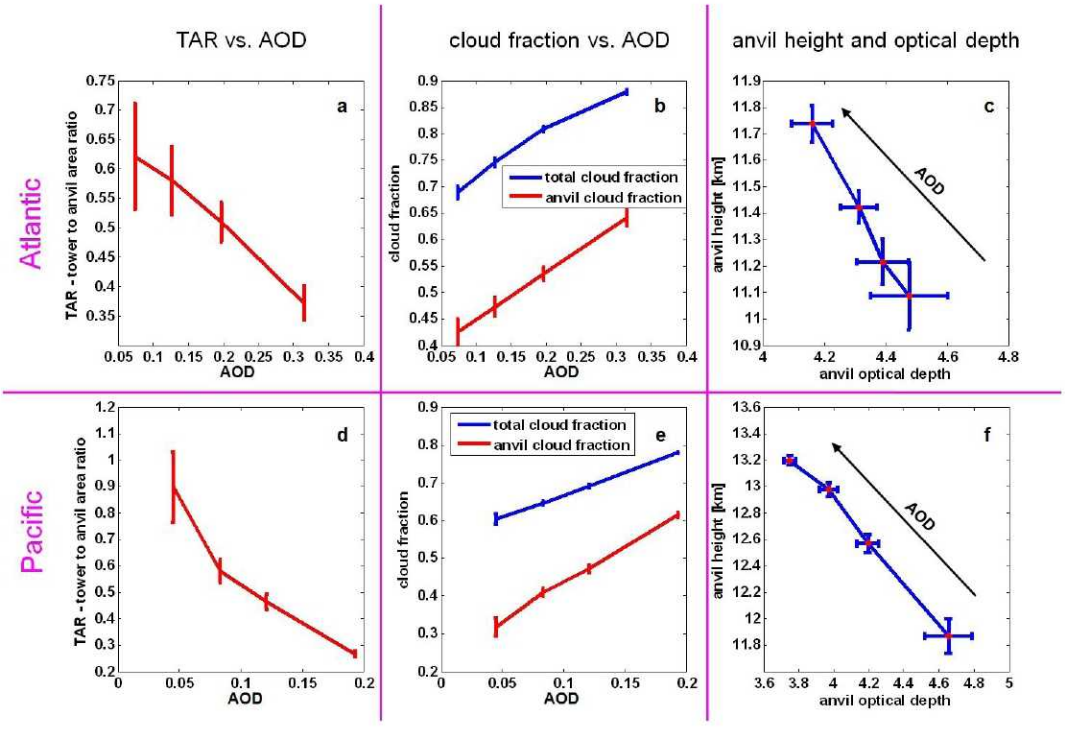

Fig. 3. Relationships between deep convective cloud characteristics and aerosol loading. Top row refers to the Atlantic study region (0° N to 14° N; 18° W to 45° W). Bottom row refers to the Pacific study region (0° N to 14° N; 180° W to 150° W). Left column – **(a)** and **(d)**, tower to anvil area ratio as a function of aerosol optical depth (AOD). Center column – **(b)** and **(e)**, cloud fraction as a function of AOD. The blue curve shows the total cloud fraction. The red shows only the anvil cloud fraction. Note the similarity in slopes. The change of total cloud fraction with aerosol is driven by the expansion of the anvils, and the decrease in the relative contribution of the towers. Right column, **(c)** and **(f)**, anvil height and anvil optical depth for the four levels of aerosol loading marked in left figures. The low level AOD is associated with the lower right dot. The black arrow marks the AOD increase direction. Increase in aerosol loading is associated with increase of anvil height and with a decrease in anvil optical depth or a thinning of the anvil as it spreads out.

stretches the anvils to cover a larger area, the ice path is diluted in the process, resulting in a smaller TAR (Fig. 3a and d) and a decrease in anvil optical depth (Fig. 3c and f).

2.2 Top of the atmosphere forcing estimations – introducing the τ-Z cloud forcing space

How does such a chain of events affect the climate radiative forcing? Clouds cool the atmosphere by reflecting back to space part of the incoming shortwave solar radiation. They warm the atmosphere by absorbing longwave radiation emitted from the surface and lower atmosphere, and therefore, reduce the thermal energy loss to space. These two different radiative processes depend on different cloud properties. The longwave cloud radiative effect depends on cloud temperature and emissivity. Cloud temperature is linked to the height and physical thickness of the cloud, and the local profile of air temperature. Cloud emissivity is linked to cloud liquid water content, but saturates quickly so that cloud emissivity is mostly constant for a wide range of cloud optical depths. The important point is that higher clouds with colder cloud top temperatures will emit less longwave radiation to space, thereby warming the atmosphere. In the solar range cloud height plays a minor role and the liquid water/ice content, cloud optical depth, droplet size distribution and thermodynamic phase are the critical cloud parameters that determine cloud reflectance of solar radiation. Liquid water content is not measured directly from passive remote sensing but can be estimated as the product of the cloud optical thickness τ and cloud effective radius r_e, (which is the ratio of the 3rd and 2nd moments of the droplet size distribution). Both τ and r_e are retrieved simultaneously from spectral reflectance measurements using one visible channel and one channel in the mid-infrared (Nakajima and King, 1990; Platnick et al., 2003). Optically thicker clouds with smaller droplets/ice particles will reflect more shortwave radiation back to space. The net radiation effect is a superposition of the longwave and shortwave processes.

The different sensitivity of the solar and thermal radiative regimes to cloud properties implies different response in terms of radiative forcing. To demonstrate the sensitivity of the top-of-the-atmosphere (TOA) forcing to the deep convective cloud properties we introduce the τ-Z cloud forcing space in which each point on this space represents the TOA

forcing per cloud top height (vertical axis Z) and cloud optical depth (horizontal axis τ).

Cloud shortwave reflectance depends not only on the cloud optical depth (as presented in the τ-Z space) but also on the clouds' droplet effective radius and phase (water or ice). Cloud r_e will be smaller in polluted conditions due to higher concentrations of cloud condensation nuclei (CCN), but will increase with height in the cloud. Cloud drop freezing (thermodynamic phase) depends on the temperature, the ice nuclei concentration and the size of the drops. It was shown that higher CCN concentration produce smaller water drops and by that delay the freezing level to higher altitude and colder temperature (Rosenfeld and Woodley, 2000).

Figure 4a shows the τ-Z space of a deep convective tropical cloud. It shows the daily average net radiative forcing calculated using the Santa Barbara DISTORT Atmospheric Radiative Transfer Model (SBDART, Ricchiazzi et al., 1998) for a typical tropical temperature profile, as a function of the cloud optical depth and height.

It can be seen that any transition towards the left and/or top of the τ-Z space will be translated as a positive forcing (warming). Moreover the gradients in the plane are far from being linear, suggesting that the estimation of the average forcing from different cloud elements may not be simple. To illustrate the above point in a very simple example, Figure 4b shows one cross-section of the τ-Z space for $Z = 10.5$ km (marked as a dashed line in Fig. 4a). Note that the τ scale is logarithmic suggesting that the apparent linear slope on the right part of the figure is actually an exponent. Therefore, since such function is a convex function, the Jensen's inequality applies (Newman et al., 1995). If the average cloud optical depth τ_c in a pixel equals the normalized by area average of all the clouds in the pixel, the overall cloud forcing of this pixel will be larger than the forcing of the average cloud. As an example, say that within a given pixel all of the clouds tops are at $Z = 10.5$ km. Say that a cloud with one area element has optical depth $\tau_t = 44$ and another cloud occupies 9 area elements with $\tau_a = 4$. Therefore $\tau_c = 8$ and from Fig. 4b one can see that the corresponding forcing in the cloudy area with $Z = 10.5$ km and $\tau_c = 8$ would be $F = \sim 5$ W/m^2 (the magenta line in Fig. 4b). In fact the true forcing will be the normalized by area average of the forcing namely (9·35–1·68)/10=24 W/m^2 (see the red lines in Fig. 4b) almost 5 times larger than the forcing of the average.

The sensitivity of the τ-Z space on r_e is demonstrated in Fig. 5. Roughly it shows that the zero forcing line marking the transition from negative forcing (cooling, cold colors) to positive (warming, hot colors) occurs higher in the atmosphere for larger r_e, suggesting that for a given τ the shift to warming will occur in lower clouds in polluted conditions. The zero forcing line occurs at lower levels for ice as compared to water (for a given τ and r_e) suggesting that delay in freezing will delay the transition to warming.

For the τ-Z space used in Fig. 4, we chose a combination of parameters that will mark the higher (conservative) boundaries from cooling to warming, and will accentuate the cloud cooling regime. The transition to ice is delayed until close to −40 °C for complete freezing and the effective radius profile is skewed towards large droplets and crystals, from 20 µm in the lower cloud to 40 µm at higher levels.

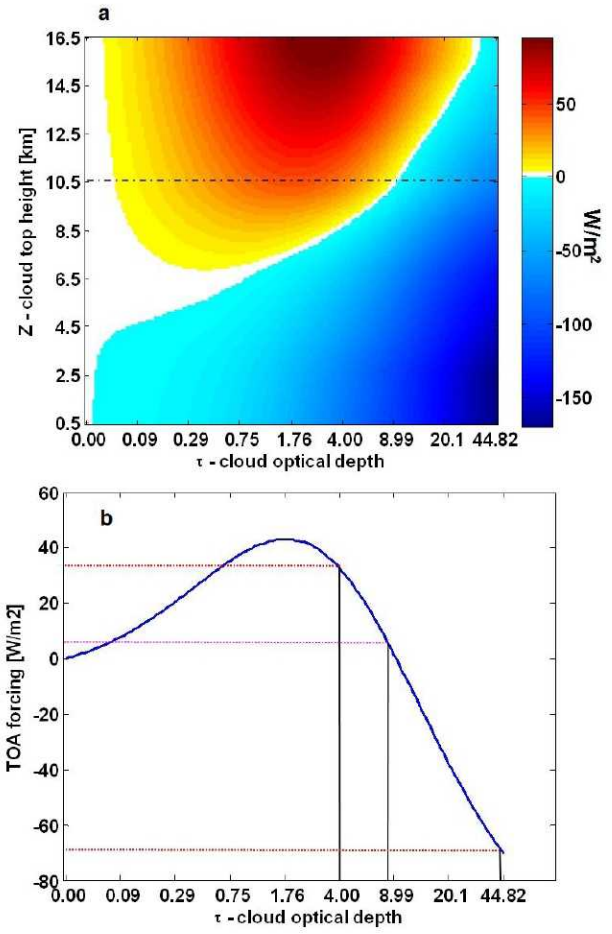

Fig. 4. Upper: τ-Z space of the cloud radiative forcing at the top of the atmosphere, where τ denotes the cloud optical depth and Z, the cloud top altitude. The color indicate the top of the atmosphere (TOA) daily average cloud radiation effect in [W/m^2] as a function of the cloud height (vertical axis) and cloud optical depth (horizontal axis) for average effective radius ranging from 20 to 40 µm in the upper atmosphere and mixed phase starting from −20 ° to −40 °C where full freezing occurs. Warm colors represent a net warming effect, white represents zero net effect and cold colors represent net cooling. Any shift of the clouds to the left and/or up in the τ-Z space is associated with a shift toward warming. Note how complex the space is, suggesting that averaging of cloud properties (τ and Z) will result in wrong radiative flux estimations. Lower: cross section taken from the above τ-Z space at Z=10.5 km, showing top-of-atmosphere (TOA) forcing as a function of cloud optical depth. The bottom figure demonstrates that the mean forcing of anvils with τ=4 (35 Wm^{-2}), covering 90% of the scene, and towers with τ=44 (−68Wm^{-2}), covering 10% of the scene is ∼25 Wm^{-2}, is 5 times higher than the forcing calculated for the mean τ of the scene τ=8, (5 Wm^{-2}).

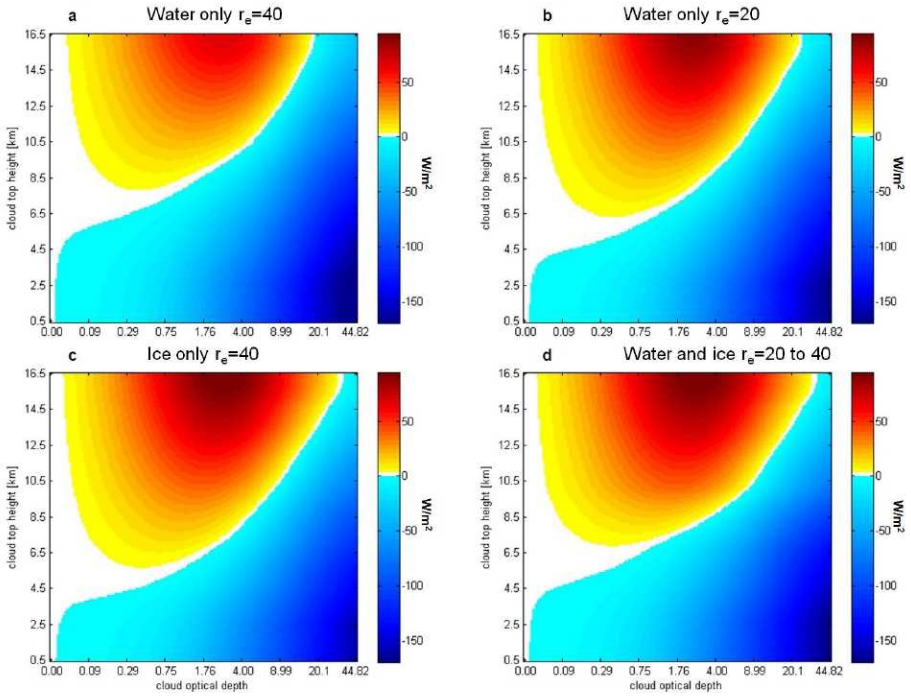

Fig. 5. Sensitivity of the cloud τ-Z space to the cloud thermodynamic phase and the effective radius of the cloud particles (r_e). **(a)** Water clouds with r_e=40 μm. **(b)** Water clouds with r_e=20 μm. **(c)** Only ice particles with r_e=40 μm. **(d)** Corresponds to Fig. 3 with mixed phase and a range of particle sizes from r_e=20 μm at low altitudes to 40 μm at upper altitudes. The white color represents the zero net forcing and marks the transition from negative forcing (cooling, cold colors) to positive (warming, hot colors). Following the location of the transition zone reveals that the tendency is for the warming effect to extend to lower altitudes for ice phase and smaller particles.

Traditionally, aerosol indirect effects are thought to be primarily cooling. Here we show that by enhancing anvil development, the result can be significant warming instead.

3 Discussion

3.1 Retrieval artifacts and meteorology

When studying cloud aerosol interactions from observations two inherent problems will always surface, namely 1) cloud contamination effects on the aerosol retrievals and 2) cause and effect – separation of true net aerosol effects on clouds from meteorological effects driving both aerosol and clouds.

On one hand one wants to measure aerosol as close as possible to clouds in order to truly reflect the relevant aerosol (that interacts with the clouds) properties. On the other hand, one asks for very accurate measurements of aerosol loading and properties, which are very difficult to achieve in the vicinity of clouds (Koren et al., 2007, 2008b; Charlson et al., 2007; Wen et al., 2007). Even if assuming that one can measure correctly clouds and aerosol in a cloud field, the next challenge is due to the strong coupling of both to meteorology (environmental properties). Are the trends seen between aerosol loading and cloud anvils due to real aerosol effects on clouds, or does the meteorology drive the changes in both aerosol and cloud properties?

The question of decoupling the meteorology from the net aerosol effect was tackled in Koren et al. (2005). There, they suggested that vertical velocity from a reanalysis model can serve as a good proxy for deep convection. By dividing the data to subsets with similar vertical velocity (magnitude and sign) and analyzing each set separately they showed that the aerosol effect of invigoration of the convective clouds is true for any of the subsets.

A recent study was conducted with the objective of providing deeper and detailed answers to these two key questions over the same study area (Koren et al., 2010). It shows that even after rejection of most of the pixels that may contain cloud contamination, the trends between aerosol and clouds are kept. Moreover, cloud properties as a function of aerosol loading show similar trends when using the Goddard Chemistry Aerosol Radiation and Transport (GOCART) model (Chin et al., 2000) as a measure for the aerosol loading (instead of satellite measurements). Moving on from the question of cloud contamination in the aerosol data set to the question of separating meteorology from aerosol effects, the study analyzed 280 meteorological variables to see which variables best represent the properties of deep convective clouds measured from space. The selected variables

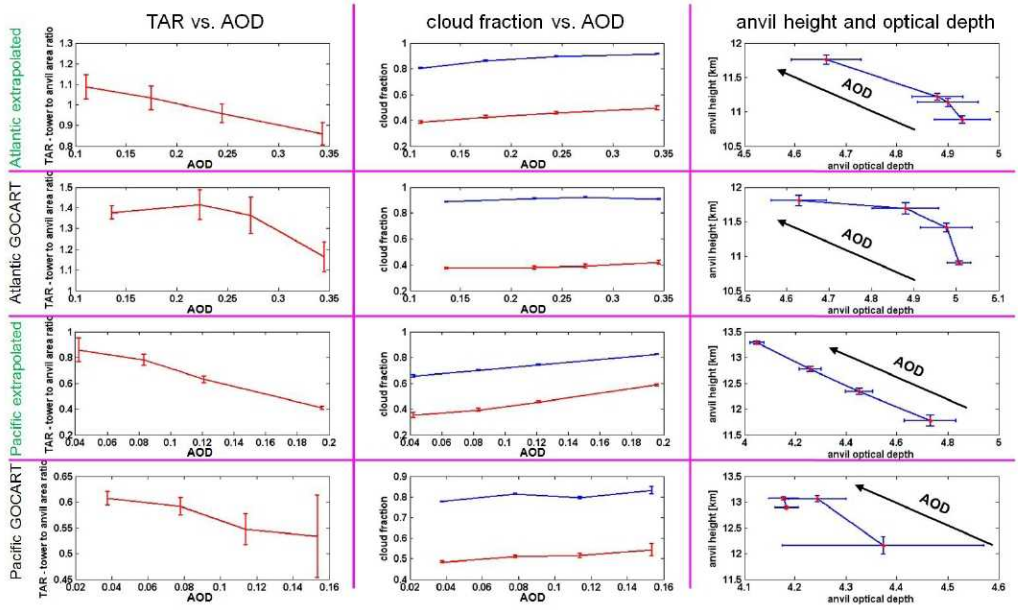

Fig. 6. Same as Fig. 3 except for using two alternative methods to determine aerosol loading. The first and third rows use the MODIS AOD data but extrapolate from retrieved grid boxes into fully overcast grid boxes that did not contribute to the statistics of Fig. 3. The first and second rows show results of the Atlantic set and the third and forth show results of the Pacific. This method allows inclusion of the tallest, most invigorated convective systems. The second and fourth rows use the GOCART chemical transport model (Chin et al., 2000) to provide the aerosol information that is collocated with the satellite-retrieved cloud variables. The trends exhibited by these two alternative methods are the same as shown in Fig. 3, demonstrating the robustness of the phenomena described.

helped to divide the data into subsets that represent different meteorological conditions. Convective clouds and aerosol analysis were conducted per each meteorological state showing similar aerosol effects for all the sets.

3.2 Fully overcast pixels

An additional limitation of this study is related to the necessity of having both clouds and aerosol information in the same region. As cloud cover approaches full overcast conditions, aerosol retrievals become rare. Such is the case with the most vigorous convection having the broadest spread of anvils. This may suggest that our analysis is biased to the boundaries of the developed clouds and that we may miss part of the more developed clouds that are away from the borders. Such limitation may result in underestimation of the clouds invigorated by aerosols into the higher atmosphere warming regime of τ-Z space (Fig. 4a). In order to check this we extrapolated the AOD data to pixels with no data as long as they are adjacent to at least one pixel with data. Therefore we are estimating the AOD of pixels obscured by clouds by averaging the AOD of their neighbour pixels with AOD retrievals. Moreover similarly to Koren et al., 2010, the anvil analyses was re-done using GOCART aerosol transport model information (Chin et al., 2000) as a measure of the aerosol loading (instead of the satellite measurements).

Figure 6 shows both extrapolated and GOCART analysis for the Atlantic and the Pacific in a similar manner to Fig. 3. The overall trend of the tower to anvil ratio, the cloud fractions and the cloud height is similar for the extrapolated data and nosier for the GOCART. Note that for the Atlantic data the TAR is larger for the extrapolated data suggesting that the non-extrapolated data underestimate the cloud thickness. However, this is not the case for the Pacific data.

Histograms of cloud fraction (right) and cloud top height (left) over the Atlantic study area are plotted in Fig. 7. It shows the distributions of all cloudy pixels (red) vs. the ones that have both aerosol and cloud information (blue). When using the AOD pixels without extrapolation (upper row) the analysis misses a significant part of the high clouds with the larger cloud fraction. Based on the cloud top height (left) histogram it can be seen that most of the effect of the high clouds (warming effect) is likely not to be included in such analysis. When using the extrapolated data (lower row) a greater portion of pixels with large cloud fraction is included increasing significantly the contribution of high clouds.

3.3 Restricting meteorological variance

It is suggested in Koren et al. (2010) that the most important meteorological variables with respect to spanning the variance of deep convective clouds over the Atlantic are the broad-scale vertical velocity at mid troposphere (ω

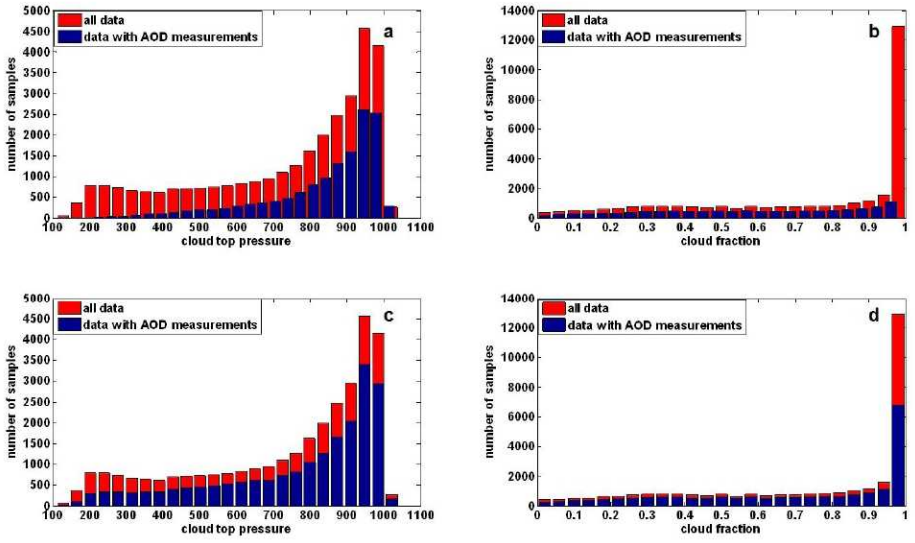

Fig. 7. Histograms of cloud fraction (right) and cloud top height (left) over the Atlantic study area. Red shows all data and blue shows pixels that have both cloud and aerosol information. The upper row shows data used for the analysis using the MODIS AOD without extrapolation (Fig. 3) and the lower row shows data with extrapolation (Fig. 6). It shows how the extrapolation (done only in cases where the adjacent neighbour has a valid AOD retrieval) of overcast pixels adds significantly to increasing the number of high clouds in the analysis (Fig. 7c).

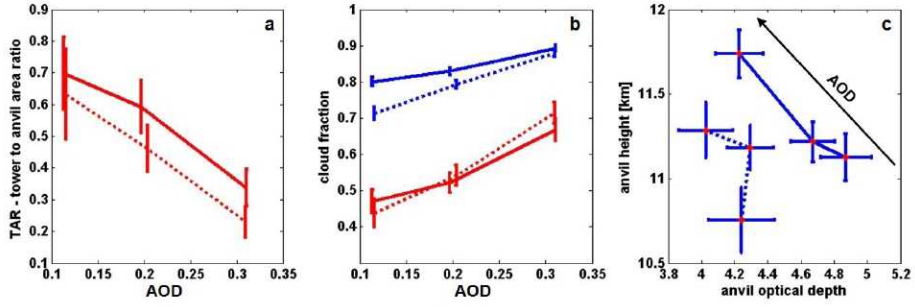

Fig. 8. Same analysis as shown in Fig. 3, but dividing the data into two meteorological regimes defined as either large scale rising motion (negative pressure vertical velocity, ω) and denoted as solid curves, or subsidence (positive ω) shown as dotted curves.

550 hPa) and the relative humidity in the upper atmosphere (RH 350 hPa). Based on this, here we restrict meteorological variance using the mid-tropospheric vertical velocity from the NOAA-NCEP Global Data Assimilation System (GDAS, Kanamitsu, 1989; Parrish and Derber, 1992). Figure 8 shows the analysis of Atlantic data similarly to Fig. 3, but the data is divided into two sets with positive (dotted) and negative vertical velocity. Note that ω is defined as a pressure vertical velocity so that negative values imply rising motion and positive values denote subsidence. Figure 8 shows that indeed the clouds with negative ω are more developed, taller and cover larger areas. It is also shown that the aerosol effect is almost orthogonal to the meteorological subsetting. The same trends exist between the TAR and cloud fraction with AOD, and that the effect of the meteorology is a simple offset of the trend line. The trend in anvil optical depth (Fig. 8c) is less profound for the positive ω set.

4 Summary

In numerous climate studies cloud aerosol interaction is shown to have the potential to be a key contributor to the radiative forcing (see Heintzenberg and Charlson (2009) for detailed information). Small changes in the cloud shape, structure or lifetime can change significantly the local radiative balance.

Here we suggest that since the wind speed increases significantly in the upper atmosphere, if indeed aerosols invigorate deep convective clouds, such invigoration will have the following consequences: invigorated convection associated with increased aerosol loading results in expanded anvil spatial coverage and reduced anvil optical depth in higher levels of the atmosphere. These thinner, colder clouds might induce strong climate warming.

We introduced the τ-Z space of cloud forcing and showed that such forcing representation reveals the opposing effects and the different sensitivity on cloud properties of the solar vs. the thermal spectral regimes. Moving left in the diagram – towards lower τ, or up – towards higher altitudes indicates transition to warming. The aerosol effect suggested in this paper is moving clouds both left and up in the τ-Z space. Moreover, we have shown a more general problem in cloud forcing estimations namely since the forcing dependence on both the cloud optical depth (τ) and height (Z) is a convex function in a significant portion of the space, the forcing of the averages (τ or Z) is much smaller than the average forcing suggesting forcing underestimation at any scale other than that of the individual cloud type. In particular the τ-Z space suggests that the anvil and the tower have to be treated independently for the forcing calculations.

The limitations of such analysis were discussed. In short, we try to study aerosol interaction on deep convective clouds while knowing that measuring aerosol properties in the vicinity of such clouds is challenging. We devote a whole study specifically to examine such problems (Koren et al., 2010). Here we find the same associations between aerosol and convective cloud characteristics in two different geographical locations with entirely different aerosol transport and different oceanic surface characteristics. We find these same associations using two different methods to collocate aerosol and cloud properties and when we restrict meteorological variance. We even find the same relationships between aerosol and convective cloud properties when we use a model to provide the aerosol loading information. The results of this study are reproducible and robust, and suggest strongly that the proposed trend is a true aerosol effect.

Due to data limitations however, we do not quantify the radiative forcing of the proposed mechanism. Though critically important, reliable estimation of the radiative forcing due to aerosol effects on deep convective clouds and their anvils will have to be done by using a more complete set of information on clouds, aerosol and meteorology, in conjunction with models. Here we demonstrate a pathway of aerosol effects on clouds that can lead to a positive climate forcing. This is an important mechanism that will be required in future estimates of climate change.

Acknowledgements. I. K. would like to thank A. Kostinski for helpful comments on the research. This research was supported in part by the Minerva Foundation, the Weizmann-Argentina Cooperation program, the Yeda-Sela program and the NASA's Interdisciplinary Sciences Program under the direction of Hal Maring. I. K. is incumbent of the Benjamin H. Swig and Jack D. Weiler career development chair.

Edited by: J. H. Seinfeld

References

Albrecht, B. A.: Aerosols, cloud microphysics and fractional cloudiness, Science, 245, 1227–1230, 1989.

Andreae, M. O., Rosenfeld, D., Artaxo, P., Costa, A. A., Frank, G. P., Longo, K. M., and Silva-Dias, M. A. F.: Smoking rain clouds over the Amazon, Science, 303, 1337–1342, 2004.

Charlson, R. J., Ackerman, A. S., Bender, F. A.-M., Anderson, T. L., and Liu, Z.: On the climate forcing consequences of the albedo continuum between cloudy and clear air, Tellus B, 59, 715–727, doi:10.1111/j.1600-0889.2007.00297.x, 2007.

Chin, M., Rood, R. B., Lin, S.-J., Muller, J. F., and Thompson, A. M.: Atmospheric sulfur cycle in the global model GOCART: model description and global properties, J. Geophys. Res., 105(D20), 24671–24687, doi:10.1029/2000JD900384, 2000.

Devasthale, A., Kruger, O., and Grassl, H.: Change in cloud top temperatures over Europe, IEEE Geosci. Remote Sci., 2(3), 333–336, 2005.

Fridlind, A. M., Ackerman, A. S., Jensen, E. J., Heymsfield, A. J., Poellot, M. R., Stevens, D. E., Wang, D., Miloshevich, L. M., Baumgardner, D., Lawson, R. P., Wilson, J. C., Flagan, R. C., Seinfeld, J. H., Jonsson, H. H., VanReken, T. M., Varutbangkul, V., and Rissman, T. A.: Evidence for the predominance of mid-tropospheric aerosols as subtropical anvil cloud nuclei, Science, 304(5671), 718–722, 2004.

Heintzenberg, J. and Charlson, R. J. (eds.): Clouds in the perturbed climate system: their relationship to energy balance, atmospheric dynamics, and precipitation, Struengmann Forum Report, vol. 2., The MIT Press, Cambridge, MA, USA, 2009.

Jacobson, M. Z., Kaufman, Y. J., and Rudich, Y.: Examining feedbacks of aerosols to urban climate with a model that treats 3-D clouds with aerosol inclusions, J. Geophys. Res., 112, D24205, doi:10.1029/2007JD008922, 2007.

Jenkins, G. S. and Pratt, A.: Saharan dust, lightning and tropical cyclones in the eastern tropical Atlantic during NAMMA-06, Geophys. Res. Lett., 35, L12804, doi:10.1029/2008GL033979, 2008.

Jenkins, G. S., Pratt, A. S., and Heymsfield, A.: Possible linkages between Saharan dust and tropical cyclone rain band invigoration in the Eastern Atlantic during NAMMA-06, Geophys. Res. Lett., 35, L08815, doi:10.1029/2008GL034072, 2008.

Kanamitsu, M: Description of the NMC global data assimilation and forecasting system, Weather and Forecast., 4, 334–342, 1989.

Kaufman, Y. J. and Koren, I.: Smoke and pollution aerosol effect on cloud cover, Science, 313, 655–658, doi:10.1126/1126232, 2006.

Khain, A. P., BenMoshe, N., and Pokrovsky, A.: Factors determining the impact of aerosols on surface precipitation from clouds: an attempt at classification, J. Atmos. Sci., 65, 1721–1748, 2008a.

Khain, A., Cohen, N., Lynn, B., and Pokrovsky, A.: Possible aerosol effects on lightning activity and structure of hurricanes, J. Atmos. Sci., 65, 3652–3677, 2008b.

King, M. D., Menzel, W. P., Kaufman, Y. J., Tanre, D., Gao, B.-C., Platnick, S., Ackerman, S. A., Remer, L. A., Pincus, R., and Hubanks, P. A.: Cloud and aerosol properties, precipitable water, and profiles of temperature and humidity from MODIS, IEEE T. Geosci. Remote, 41, 442–458, 2003.

Koren, I., Kaufman, Y. J., Resonfeld, D., Remer, L. A., and Rudich, Y.: Aerosol invigoration and restructuring of

Alantic convctive clouds, Geophys. Res. Lett., 32, L14828, doi:10.1029/2005GL023187, 2005.

Koren, I., Remer, L. A., Kaufman, Y. J., Rudich, Y., and Martins, J. V.: On the twilight zone between clouds and aerosols, Geophys. Res. Lett., 34, L08805, doi:10.1029/2007GL029253, 2007.

Koren, I., Martins, J. V., Remer, L. A., and Afargan, H.: Smoke invigoration versus inhibition of clouds over the Amazon, Science, 321, 946–949, 2008a.

Koren, I., Oreopoulos, L., Feingold, G., Remer, L. A., and Altaratz, O.: How small is a small cloud?, Atmos. Chem. Phys., 8, 3855–3864, doi:10.5194/acp-8-3855-2008, 2008b.

Koren I., Feingold, G., and Remer, L.: Deep convective clouds invigoration over the Atlantic: aerosol effect, meteorology or retrieval artifacts? Atmos. Chem. Phys., submmited, 2010.

Nakajima, T. and King, M. D.: Determination of the optical thickness and effective particle radius of clouds from reflected solar radiation measurements. Part 1: Theory, J. Atmos. Sci., 47, 1878–1893, 1990.

Newman, W. I., J. K. Lew, G. L. Siscoe, and R. G. Fovell: Systematic effects of randomness in radiative transfer. J. Atmos. Sci, 52, 427–435, 1995.

Lindsey, D. T. and Fromm, M.: Evidence of the cloud lifetime effect from wildfire-induced thunderstorms, Geophys. Res. Lett., 35, L22809, doi:10.1029/2008GL035680, 2008.

Parrish, D. F. and Derber, J. C.: The National Meteorological Center's spectral statistical interpolation analysis system. Mon. Weather Rev., 120, 1747–1763, 1992.

Platnick, S., King, M. D., Ackerman, S. A., Menzel, W. P., Baum, B. A., Riedi, J. C., and Frey, R. A.: The MODIS cloud products: algorithms and examples from terra, IEEE T. Geosci. Remote, 41(2), 459–473, 2003.

Remer, L., Kleidman, R. G., Levy, R. C., Kaufman, Y. 5 J., Tanre', D., Mattoo, S., Martins, J. V., Ichoku, C., Koren, I., Yu, H., and Holbenet, B. N.: Global aerosol climatology from the MODIS satellite sensors, J. Geophys. Res., 113, D14S07, doi:10.1029/2007JD009661, 2008.

Ricchiazzi, P., Yang, S. R., Gautier, C., and Sowle, D.: SBDART: a research and teaching software tool for plane-parallel radiative transfer in the Earth's atmosphere, B. Am. Meteorol. Soc., 79(10), 2101–2114, 1998.

Rosenfeld, D.: Suppression of rain and snow by urban and industrial air pollution, Science, 287, 1793–1796, 2000.

Rosenfeld, D. and Woodley, W. L.: Deep convective clouds with sustained supercooled liquid water down to −37.5°C, Nature, 405, 440–442, 2000.

Twomey, S.: The influence of pollution on the shortwave albedo of clouds, J. Atmos. Sci., 34, 1149–1152, 1977.

Wen, G., Marshak, A., Cahalan, R. F., Remer, L. A., and Kleidman, R. G.: Three-dimensional aerosol-cloud radiative interaction observed in collocated MODIS and ASTER images of cumulus cloud fields, J. Geophys. Res., 112, D13204, doi:10.1029/2006JD008267, 2007.